

# Mechanical Properties of Silk Fibroin–Microcrystalline Cellulose Composite Films

Yasutomo Noishiki,<sup>1</sup> Yoshiharu Nishiyama,<sup>1</sup> Masahisa Wada,<sup>1</sup> Shigenori Kuga,<sup>1</sup> Jun Magoshi<sup>2</sup>

<sup>1</sup>Department of Biomaterials Science, Graduate School of Agricultural & Life Sciences, The University of Tokyo and CREST, JST, Yayoi 1-1-1, Bunkyo-ku, Tokyo 113-8657, Japan

<sup>2</sup>National Institute of Agricultural Sciences and CREST, JST, Tsukuba, Ibaraki 305-8602, Japan

Received 11 September 2001; accepted 24 April 2002

**ABSTRACT:** Silk fibroin–microcrystalline cellulose (cellulose whisker) composite films with varied compositions were prepared by casting mixed aqueous solution/suspensions of the two components. Silk fibroin was dissolved in 10M LiSCN followed by dialysis; a cellulose whisker suspension was prepared by sulfuric acid hydrolysis of tunicate cellulose. Macroscopically homogeneous films were obtained at all mixing ratios. While the Young's modulus of the composite films showed a linear, additive dependence on the mixing ratio, the tensile strength and ultimate strain showed a maximum at a 70–80% cellulose content, reaching five times those of fibroin-alone or cellulose-alone films. At

the same mixing ratio, infrared spectra of the composite films showed a shift of the amide I peak from 1654 to 1625  $\text{cm}^{-1}$ , indicating the conformational change of fibroin from a random coil to a  $\beta$  structure (silk II) at the whisker–matrix interface. This change seems to be induced by contact of fibroin molecules with a highly ordered surface of cellulose whisker. © 2002 Wiley Periodicals, Inc. *J Appl Polym Sci* 86: 3425–3429, 2002

**Key words:** nanocomposites; crystal structures; biopolymers; mechanical properties; thin films

## INTRODUCTION

Silk fibroin is the protein constituting silk fibers produced by the silkworm. Its uniqueness is believed to arise from the glycilalanil (GlyAla) repeats, which tend to form the  $\beta$  structure under certain conditions.<sup>1</sup> Silk fibroin is known to form mainly three kinds of conformations: silk I with a helical conformation, silk II with an antiparallel  $\beta$ -sheet, and a random coil without definite orders. Silk I is the form in native glandular silk, and silk II is the form in spun silk fiber.<sup>1</sup> Besides the conventional uses as fibers, silk fibroin is finding uses in regenerated forms as medical materials, food ingredients, and other specialty uses.<sup>2,3</sup>

Cellulose,  $\beta$ -1,4-glucan, is another abundant natural polymer. It is usually produced as crystalline microfibrils with widths of 3.5–30 nm depending on the origin.<sup>4</sup> Acid treatment of native cellulose results in disruption of microfibrils and formation of rodlike crystallites (whiskers).<sup>5</sup> Since the cellulose crystal has a high Young's modulus [approximately 100 GPa (ref. 6)], use of cellulose whiskers as a component of nano-

composite materials has been explored in combination with poly(vinyl chloride)<sup>7,8</sup> and latex.<sup>9,10</sup>

While several attempts have been reported on the preparation of cellulose–silk fibroin composites,<sup>11,12</sup> they involved molecular blending of the two components, that is, through solubilization of fibroin and cellulose by certain aqueous cosolvents. In the light of the remarkable mechanical properties of cellulose whisker, we examined here the effect of combining it with silk fibroin in an aqueous media in terms of mechanical strength and the influence on the higher-order structure of silk fibroin.

## EXPERIMENTAL

### Samples

#### Silk fibroin

Silk cocoon (*Bombix mori*) was degummed (removal of sericine) by boiling in a 0.3% (w/v) sodium dodecylsulfate and 0.06% (w/v) sodium carbonate solution for 1 h. After rinsing with boiling water, the sample was washed in methanol and dried at room temperature.<sup>13</sup> Three grams of degummed silk fibroin was dissolved in 25 mL of 10M lithium thiocyanate (LiSCN), by keeping the mixture at room temperature for 1 h, then at 50°C for 1 h. The solution was passed through a filter paper and desalted by dialysis in

Correspondence to: Y. Noishiki (noishiki@sbp.f.a.u-tokyo.ac.jp).

cellulose tubing against water. This solution, however, was unstable and slowly formed a precipitate by standing at room temperature for several days; therefore, the solution was freshly prepared before the composite film preparation each time. The solid content of the aqueous solution (approximately 2%) was determined gravimetrically by drying it.

#### Cellulose whisker

Mantles of tunicate, obtained at a local fish market, were slit open and soaked overnight in 5% (w/v) KOH at room temperature. The sample was rinsed with water, treated with 0.34% (w/v) NaClO<sub>2</sub>, and thoroughly rinsed with water.<sup>14</sup> The purified cellulose was hydrolyzed in 64% (w/w) sulfuric acid at 60°C overnight. The resulting microcrystals were washed by repeated centrifugation (5000 rpm, 5 min) and re-dispersion in water. The well-dispersed microcrystalline particles remaining in the supernatant after several runs of centrifugation were concentrated by centrifugation at 11,000 rpm for 1 h. After dialyzing against water, the suspension was neutralized with 0.1N NaOH to pH 7.0.

#### Preparation of composite films

The silk fibroin solution and the cellulose whisker suspension (both approximately 2% solid content) were mixed to give the desired ratios: 100/0, 90/10, 80/20, 70/30, 60/40, 50/50, 40/60, 30/70, 20/80, 10/90, and 0/100. The mixed solution was cast onto polystyrene dishes at room temperature to form approximately 5–10- $\mu\text{m}$  (for IR) or 50–100- $\mu\text{m}$  (for X-ray diffraction and tensile test)-thick films.

#### X-ray diffractometry

X-ray diffraction diagrams of the films were obtained with a rotating anode X-ray generator, RotaFlex RU-200BH (Rigaku), using nickel-filtered CuK $\alpha$  radiation ( $\lambda = 0.15418$  nm) operated at 100 mA and 50 kV. The diffraction diagrams were recorded on imaging plates (FUJIX BAS300UR, Fuji Film) and were read with a RAXIS DS3 (Rigaku).

#### FTIR

IR spectra of composite films were obtained using a Fourier transform infrared (FTIR) spectrometer, Nicolet MAGNA860, with a resolution of 4 cm<sup>-1</sup> and accumulation of 64 scans between 4000 and 400 cm<sup>-1</sup>.

#### Transmission electron microscopy

The silk fibroin solution and cellulose whisker suspension were mixed to make a solid composition of 50/50.

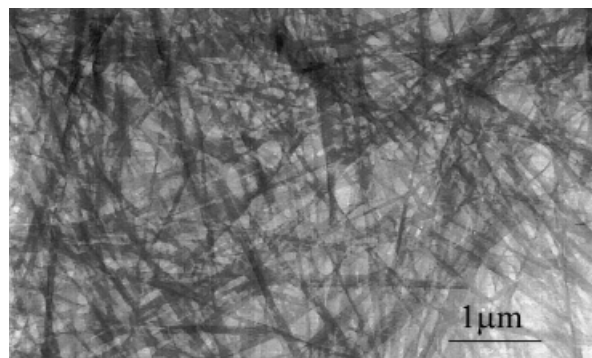


**Figure 1** Transmission electron micrograph of silk fibroin-cellulose whisker 50/50 composite.

The mixture was mounted onto a thin carbon support and examined by a transmission electron microscope, JEOL 2000EX. Images of the whiskers were recorded by defocus contrast, without staining.

#### Tensile test

Cast films were cut into 5 × 60-mm pieces. The thickness, ranging from 70–170  $\mu\text{m}$ , was determined using a micrometer. The test pieces were subjected to a tensile test using a Tensilon/UTM-III-100 (Toyo Baldwin) at 20°C and 65% RH. The head speed was 10 mm/min and the span was 50 mm.

## RESULTS AND DISCUSSION

Figure 1 shows a transmission electron micrograph of a silk fibroin-cellulose whiskers composite. While silk fibroin is not visible, whiskers are seen as well-dispersed straight rods. Because of a large axial ratio of the rods, they are forced to lie horizontally after casting, while their orientation in the plane is random. The spaces between the cellulose whiskers should be filled with silk fibroin as the matrix. The appearance of dispersed whiskers was the same for the pure cellulose sample (picture not shown). The composite films used for infrared spectroscopy and mechanical measurements are considered to consist of the same structure stacked to form a macroscopic thickness.

#### X-ray diffractometry

Figures 2 and 3 show the X-ray diffraction diagrams and corresponding intensity profiles of the composite films. The pure silk fibroin [Fig. 3(a)] gave clear reflections ( $2\theta = 12.2^\circ$  and  $19.5^\circ$ ) corresponding to 0.72- and 0.44-nm lattice spacings of silk I.<sup>15,16</sup> The pure cellulose film gave a well-defined pattern of cellulose I $\beta$  [Fig. 3(e)].<sup>17,18</sup> While the pattern of the composite films should be the superposition of those of the two components if they do not interact with each other at

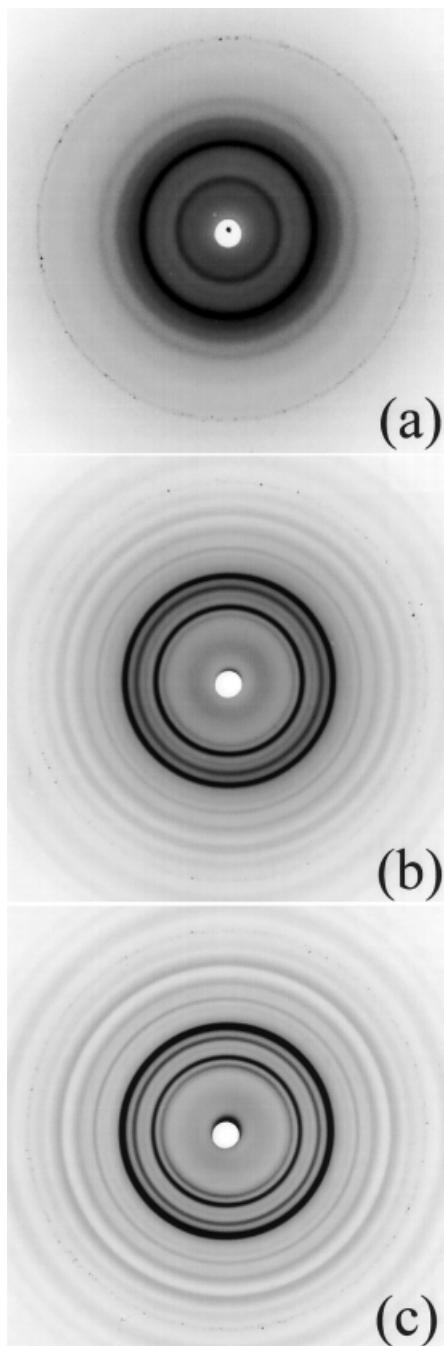
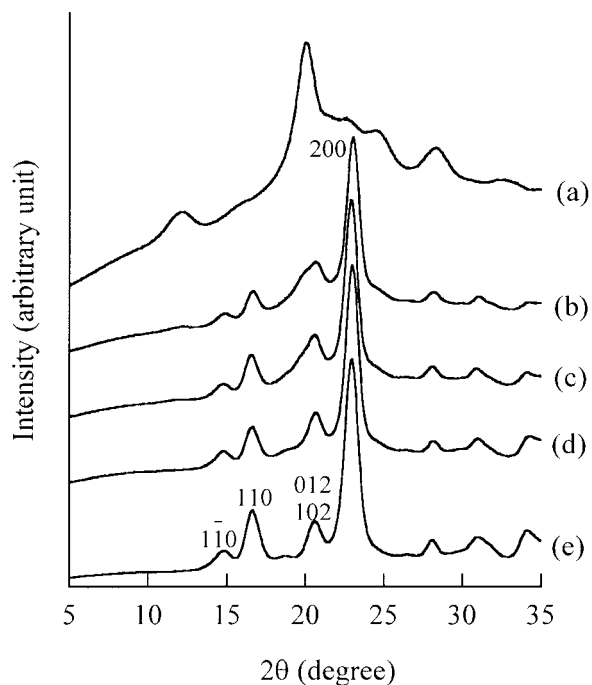


**Figure 2** X-ray diffraction patterns of (a) silk fibroin, (b) silk fibroin–cellulose whisker composite (50/50), and (c) cellulose whisker.

molecular levels, the contribution of fibroin crystal ( $12.2^\circ$  and  $19.5^\circ$ ) is not clear in the composite films [Fig. 3(b–d)], even at 70% fibroin. This implies that the presence of cellulose prevents the formation of regular fibroin crystal.

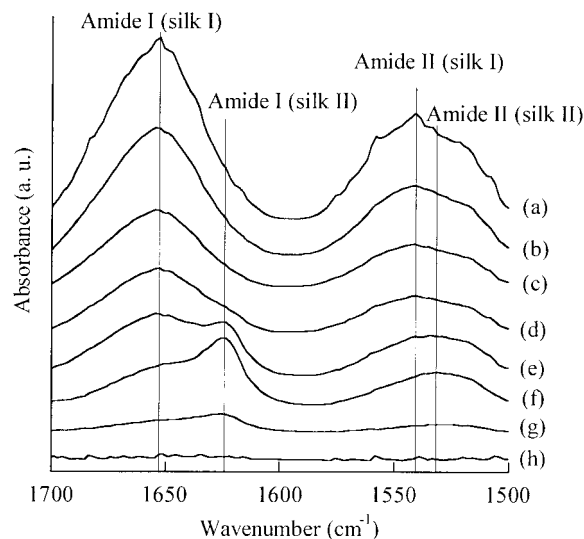
#### Infrared spectroscopy

Figure 4 shows the infrared spectra of silk fibroin, cellulose whisker, and their composite films. The band



**Figure 3** X-ray diffraction profiles of silk fibroin–cellulose whisker composite films. Silk fibroin/cellulose ratio: (a) 100/0; (b) 70/30; (c) 50/50; (d) 30/70; (e) 0/100. Unit cell conversion follows Woodcock and Sarko.<sup>17</sup>

at  $1654\text{ cm}^{-1}$  of fibroin [Fig. 4(a)] is assigned to the amide I of random coil or silk I.<sup>19,20</sup> Since cellulose has no absorption bands in this region, the series (b)–(d) in Figure 4 clearly shows a gradual decrease in the intensity of these bands according to the decrease in the fibroin content. At a fibroin content of 30–10%, however, the composite film showed a distinctive shift of the amide I band from  $1654$  to  $1625\text{ cm}^{-1}$  [Fig. 4(e–g)].



**Figure 4** Infrared spectra of fibroin–cellulose whisker composite films. Silk fibroin/cellulose ratio: (a) 100/0; (b) 80/20; (c) 60/40; (d) 40/60; (e) 30/70; (f) 20/80; (g) 10/90; (h) 0/100.

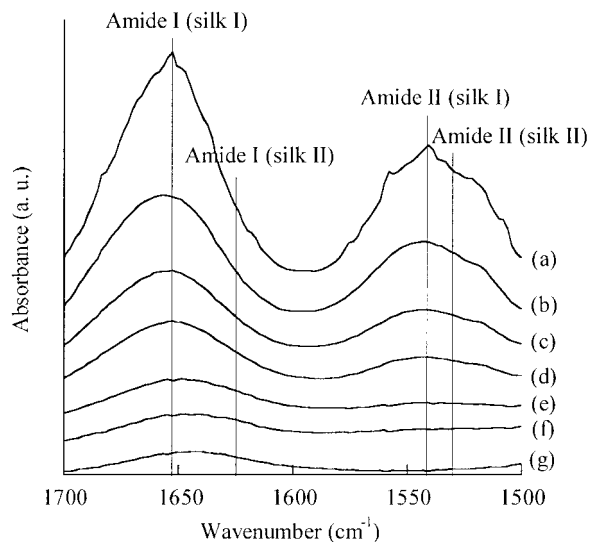


**Figure 5** Infrared spectra of fibroin–amorphous cellulose composite films. Silk fibroin/cellulose ratio: (a) 100/0; (b) 60/40; (c) 60/40; (d) 30/70; (e) 20/80; (f) 10/90; (g) 0/100.

At the same time, the amide II band at  $1540\text{ cm}^{-1}$  shifted to  $1530\text{ cm}^{-1}$ . These changes clearly show the formation of the  $\beta$  structure (silk II)<sup>16,19</sup> from the random coil state in the solution.

This result seems to contradict the result of X-ray diffraction, which showed no crystalline order of fibroin. This situation, however, can be interpreted as the formation of the  $\beta$  structure limited to the close vicinity of the whisker surface, without a three-dimensional periodicity.

A similar behavior of silk fibroin by molecular blending with chitosan has been suggested,<sup>21</sup> but the data were not clear enough because of the presence of an overlapping band from chitosan. The silk fibroin–cellulose blend films prepared from a copper–ammoniac solution as a cosolvent were shown to contain the  $\beta$ -form of silk fibroin.<sup>11,12</sup> These samples, however, were prepared in a coagulating bath containing solvents that are known to induce the  $\beta$  structure; therefore, the influence of cellulose on the structure formation of fibroin has not been clear.

To examine the influence of cellulose crystallinity, we examined the infrared spectra of a series of composite films using the same fibroin and minute particles of amorphous cellulose, which were prepared by treating Whatman CF11 cellulose powder with a 58% (w/w) calcium thiocyanate solution followed by acid hydrolysis. The resulting IR spectra (Fig. 5) did not show any shift of the amide bands of fibroin. Therefore, our results indicate that the surface of the highly crystalline cellulose exerts a characteristic influence on the conformation of fibroin that solidifies upon casting. The presence of the  $\beta$  structure in the resulting fibroin is clearly seen in the IR spectrum for a 70–90% cellulose content, but

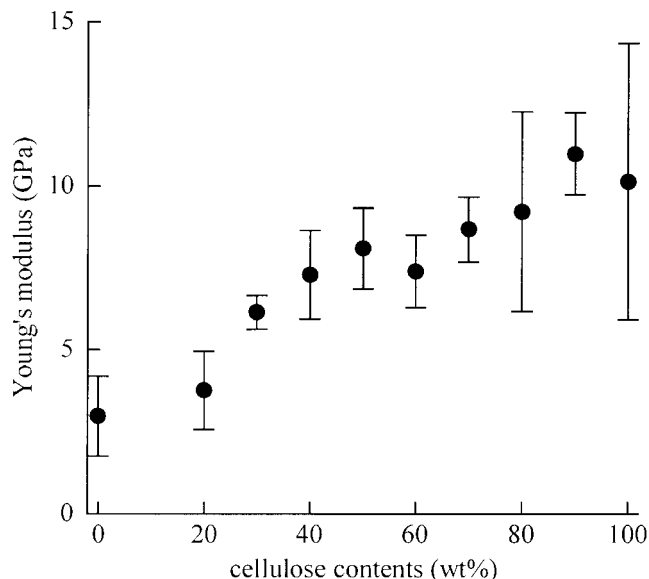


**Figure 6** Young's modulus of silk fibroin–cellulose composite films.

not for the samples with lower cellulose contents [Fig. 4(b–d)]. This is considered to be due to the reduced proportion of fibroin molecules in contact with the surface of the cellulose whiskers.

### Tensile properties

The Young's modulus of the fibroin–cellulose whisker composites showed a nearly linear dependence on the mixing ratio (Fig. 6). In contrast, the tensile breaking strength of the composite film showed an anomalous dependence on the mixing ratio (Fig. 7). While the pure fibroin and the pure cellulose films showed

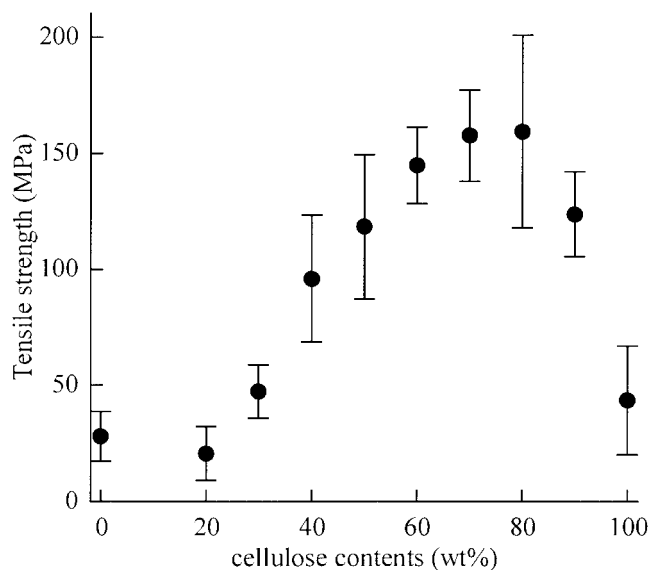


**Figure 7** Tensile strength of silk fibroin–cellulose composite films.

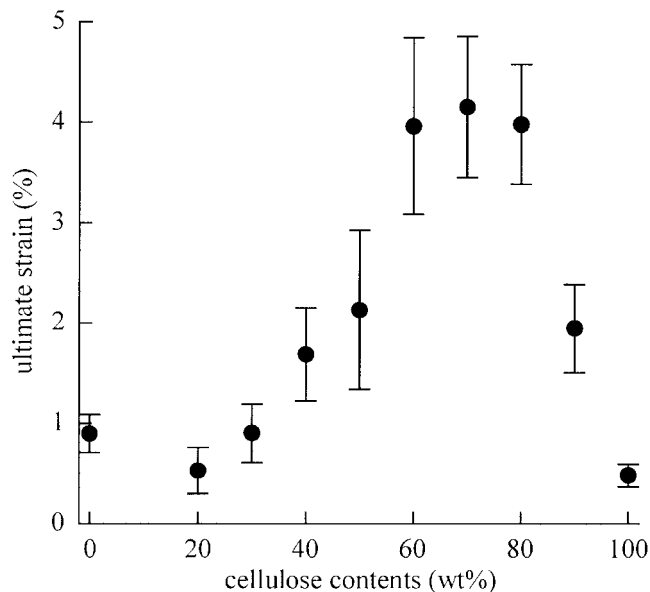


**Figure 8** Ultimate strain of fibroin-cellulose composite films.

strengths of 30–50 MPa, the composite film was remarkably stronger, reaching a maximum of approximately 160 MPa, at 70–80% cellulose content. This maximum value well exceeds those reported for silk/cellulose [45 MPa (ref. 11)] and silk/chitosan [90 MPa (ref. 22)] molecular blend films. The ultimate strain also showed a similar dependence on the mixing ratio (Fig. 8). The large deformability at 60–80% cellulose content is apparently the cause of the high breaking strengths.

Our test on the cellulose-poly(vinyl alcohol) (PVA) composite, that is, replacing silk fibroin by PVA, did not give such a strengthening effect on the composite film. Also, such an effect was not observed for the combination of regenerated cellulose particles and silk fibroin. Therefore, the described effect seems to be characteristic of the cellulose whisker-silk fibroin composite, and it is reasonable to assign this effect to the  $\beta$ -structure formation of fibroin as detected by infrared spectra. Fibroin usually forms a  $\beta$  structure only under shearing or elongating stress, but the flat and ordered surface of cellulose whisker probably serves as a template through its specific interactions with the fibroin molecules. These interactions should cause stronger adhesion between the two components, leading to the composites with greater tensile strengths.

### CONCLUSIONS

Composite films of cellulose whisker and fibroin showed improved mechanical strength at a 20–30 wt

% fibroin content, with breaking strength and ultimate strain about five times those of the constituent materials. From the observed shift in the infrared absorption bands of amide I and amide II of fibroin, the anomaly in the mechanical strength is considered to arise from the  $\beta$ -structure formation of fibroin induced by contact with the highly ordered surface of cellulose whiskers. This phenomenon is not practicable for producing bulk materials because of the lengthy procedure of solubilization and dialysis involved, but may be useful in biomedical applications such as for cell culture media and implant materials, since both components are chemically inert and known to be compatible with living tissues.<sup>1–3</sup>

### References

- Kaplan, D. L.; Mello, C. M.; Arcidiacono, S.; Fossey, S.; Senecal, K.; Muller, W. In *Protein Based Materials*; McGrath, K.; Kaplan, D., Eds.; Birkhauser: Boston, 1997; Chapter 4.
- Minoura, N.; Tsukada, M.; Nagura, M. *Biomaterials* 1990, 11, 430.
- Yamamura, K.; Kuranuki, N.; Suzuki, M.; Tanigami, T.; Matsuzawa, S. *J Appl Polym Sci* 1990, 41, 2409.
- Young, R. A. In *Cellulose*; Young, R. A.; Rowell, R. M.; Eds.; Wiley-Interscience: New York, 1986; Chapter 6.
- Fleming, K.; Gray, D. G.; Matthews, S. *Chem Eur J* 2001, 9, 7.
- Ishikawa, A.; Okano, T.; Sugiyama, J. *Polymer* 1997, 38, 463.
- Chazeau, L.; Cavaille, J. Y.; Terech, P. *Polymer* 1999, 40, 5333.
- Chazeau, L.; Cavaille, J. Y.; Canova, G.; Dendievel, R.; Bouthierin, B. *J Appl Polym Sci* 1999, 71, 1797.
- Favier, V.; Chanzy, H.; Cavaille, J. Y. *Macromolecules* 1995, 28, 6365.
- Hajji, P.; Cavaille, J. Y.; Favier, V.; Gauthier, C.; Vigier, G. *Polym Compos* 1996, 17, 612.
- Freddi, G.; Romano, M.; Massafra, M.; Tsukada, M. *J Appl Polym Sci* 1995, 56, 1537.
- Yang, G.; Zhang, L.; Liu, Y. *J Membr Sci* 2000, 177, 153.
- Agarwal, N.; Hoagland, D. A.; Farris, R. J. *J Appl Polym Sci* 1997, 63, 401.
- Sugiyama, J.; Chanzy, H.; Maret, G. *Macromolecules* 1992, 25, 4232.
- Kratky, O. *Trans Faraday Soc* 1952, 52, 558.
- Asakura, T.; Kuzuhara, A.; Tabeta, R.; Saito, H. *Macromolecules* 1985, 18, 1841.
- Woodcock, C.; Sarko, A. *Macromolecules* 1980, 13, 1183.
- Wada, M.; Sugiyama, J.; Okano, T. *J Appl Polym Sci* 1993, 49, 1491.
- Magoshi, J.; Mizuida, M.; Magoshi, Y.; Takahashi, K.; Kubo, M.; Nakamura, S. *J Polym Sci Polym Phys Ed* 1979, 17, 515.
- Hayakawa, T.; Kondo, K.; Yamamoto, S.; Noguchi, J. *Kobunshi Kagaku* 1970, 27, 300.
- Chen, X.; Li, W.; Yu, T. *J Polym Sci Part B Polym Phys* 1997, 35, 2293.
- Park, S. J.; Lee, K. Y.; Ha, W. S.; Park, S. Y. *J Appl Polym Sci* 1999, 74, 2571.